Lab on a Chip

ARTICLE

# Cross-talk between emulsion drops: How are hydrophilic reagents transported across oil phases?

Received 00th January 20xx,
Accepted 00th January 20xx

DOI: 10.1039/x0xx00000x

www.rsc.org/

Gianluca Etienne[a], Antoine Vian[a], Marjan Biočanin[b], Bart Deplancke[b], Esther Amstad[a*]

Emulsion drops are frequently used as vessels, for example, to conduct biochemical reactions in small volumes or to perform screening assays at high throughputs while consuming minimal sample volumes. These applications typically require drops that do not allow exchange of reagents such that no cross-contamination occurs. Unfortunately, in many cases, reagents are exchanged between emulsion drops even if they have a low solubility in the surrounding phase, resulting in cross-contaminations. Here, we investigate the mechanism by which hydrophilic reagents are transported across an oil phase using water-oil-water double emulsion drops as model system. Remarkably, even large objects, including 11000 base pair double-stranded circular DNA are transported across oil shells. Importantly, this reagent transport, that is to a large extent caused by aqueous drops that spontaneously form at the water-oil interface, is not limited to double emulsions but also occurs between single emulsion drops. We demonstrate that the uncontrolled reagent transport can be decreased by at least an order of magnitude if appropriate surfactants that lower the interfacial tension only moderately are employed or if the shell thickness of double emulsions is decreased to a few hundreds of nanometers.

## Introduction

Emulsion drops are often used as vessels to conduct chemical,[1,2] biochemical,[3,4] and biological screening assays at high throughputs.[2,3,5–9] To achieve a high accuracy, drops must display a narrow size distribution. Drops that fulfil this requirement can be produced with microfluidic devices.[10] Recent advances in microfluidic technologies enable the formation of monodisperse drops at a much higher throughput such that the production of these well-defined drops is not the rate limiting step anymore.[11–15] These advances make monodisperse drops well-suited containers for example for conducting screening assays. The throughput achieved in these drop-based screening assays is orders of magnitudes higher than that of assays performed in bulk and therefore costs are much lower.[3] As a result, these drop-based screening assays, that allow miniaturization and automation of biological assays, are frequently employed to characterize cells on a single cell level,[16–18] to perform directed evolution of enzymes,[3,19] single cell transcriptomics,[20,21] drug screening,[22,23] or biomarker analysis.[24–26] Drop-based screening assays are most often performed using aqueous emulsion drops that are dispersed in perfluorinated oils. These oils are selected because they are biocompatible,[27–29] have a high gas solubility,[30–32] and are compatible with polydimethylsiloxane (PDMS),[33] an elastomer commonly used to fabricate microfluidic devices. To prevent drops from coalescing, they are usually stabilized with block copolymer surfactants.[2,3,5–8,34–38] Most frequently, the surfactant is composed of two perfluorinated polyether blocks that are interspaced by a hydrophilic poly(ethylene glycol) (PEG)-based block[32,39] although alternatives with polyglycerol blocks have been reported.[40]

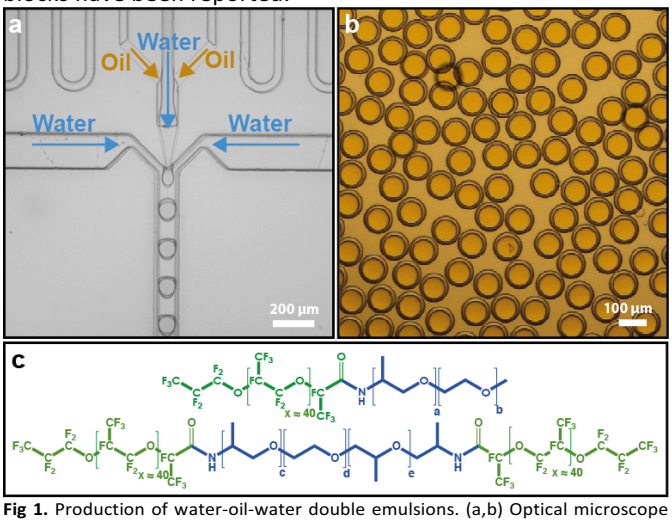


**Fig 1.** Production of water-oil-water double emulsions. (a,b) Optical microscope images of (a) a microfluidic double emulsion device in operation and (b) the resulting water-oil-water double emulsions. (c) Chemical structure of diblock (top) and triblock (bottom) copolymer surfactants with varying lengths of the hydrophilic block, as summarized in Table 1.

[a] *Soft Materials Laboratory, Institute of Materials, École Polytechnique Fédérale de Lausanne (EPFL), CH-1015 Lausanne, Switzerland. E-mail: esther.amstad@epfl.ch*
[b] *Institute of Bioengineering, École Polytechnique Fédérale de Lausanne (EPFL), CH-1015 Lausanne, Switzerland and Swiss Institute of Bioinformatics, Lausanne, Switzerland*

†Electronic Supplementary Information (ESI) available: Movies of leakage from double emulsion drops at different surfactant concentrations; time-lapse photographs of nanometer sized emulsion drops forming at the oil-water interface; movie of leakage from double emulsions with thick and thin shells. See DOI: 10.1039/x0xx00000x

**Table 1.** Overview of block copolymer surfactants used to stabilize water-oil-water double emulsions. The interfacial tension, *γ*, is measured for solutions containing 2 mM of the respective surfactants. The inverse packing parameter, α', was calculated as described in the main text.

| *Name* | *Molecular Weight Hydrophilic Block [g/mol]* | *Molecular Weight PEG [g/mol]* | *Repeat Units* | CMC [mM] | γ [mN/m] | *α' [-]* |
|---|---|---|---|---|---|---|
| FSH-PEG220 | ~280 | ~220 | b=5 | ~0.5 | ~11 | 0.37 |
| FSH-Jeffamine600 | ~580 | ~40 | a=9, b=1 | ~2 | ~7 | 0.13 |
| FSH-Jeffamine1000 | ~1030 | ~840 | a=3, b=19 | ~4 | ~21 | 0.90 |
| FSH-Jeffamine2000 | ~1960 | ~260 | a=29, b=6 | ~0.3 | ~18 | 0.42 |
| $FSH_2$-PEG310 | ~370 | ~310 | d=7 | ~0.5 | ~10 | 0.23 |
| $FSH_2$-Jeffamine600 | ~640 | ~400 | c+e=3.6, d=9 | ~1 | ~3 | 0.27 |
| $FSH_2$-Jeffamine900 | ~930 | ~550 | c+e=6, d=12.5 | ~2 | ~5 | 0.34 |
| $FSH_2$-Jeffamine2000 | ~2090 | ~1720 | c+e=6, d=39 | ~0.3 | ~24 | 0.73 |

These fluorinated polyether surfactants impart good stability to emulsion drops if they are composed of solutions with low salt concentrations.[39] However, they are prone to coalescence if drops are made of solutions containing high salt concentrations, which is often the case in biological and biochemical screening assays. In these cases, it is beneficial to employ water-oil-water double emulsions that are more stable and can be stored in an aqueous environment, facilitating their handling.[41] Irrespective of the type of emulsion drops employed, the use of surfactants comes with an important disadvantage: Surfactants contribute to spontaneous exchanges of reagents between different drops that are dispersed in perfluorinated[42–49] and hydrocarbon-based oils.[48,50]

This cross-contamination reduces the accuracy of drop-based screening assays[45] and therefore limits their performance and usefulness. The degree to which reagents are exchanged depends on their composition.[49,51–53] Cross-contamination can be reduced if the viscosity of the oil is increased,[46] if sugar,[50] or bovine serum albumin (BSA)[48] is added to the aqueous phase, by lowering the surfactant concentration,[42,48] or by replacing surfactants with nanoparticles.[54] The exact mechanism by which reagents are exchanged remains to be determined. Reagents might be transported across the oil by aggregates or inverse micelles that spontaneously form if surfactants self-assemble.[42,45,48] Reagents might also be transported across the oil by aqueous drops that spontaneously form at liquid-liquid interfaces.[55–58] A better understanding of the mechanism that causes reagent exchange between emulsion drops would open up new possibilities to control it. This understanding might enable the design of tight, surfactant-stabilized emulsion drops that do not suffer from a spontaneous reagent exchange. This would result in a much higher accuracy of drop-based screening assays, thereby enabling their use for many more applications than what is currently possible.

In this paper, we investigate the exchange of reagents across the shell of water-oil-water double emulsions stabilized with different amphiphilic block copolymers. Remarkably, even reagents as large as 11000 base pair DNA strands or 100 nm diameter poly(styrene) particles are transported across a perfluorinated oil phase despite their very low solubility in the oil. Importantly, this transport is not limited to double emulsion drops but also occurs between single emulsion drops. We find that the transport rate of reagents across the oil phase scales inversely with the interfacial tension. These results suggest that small aqueous drops with diameters of the order of 100 nm spontaneously form in the oil phase and transport hydrophilic reagents across it. Because these aqueous drops are much larger than micelles, they can also carry bigger reagents across the shell of double emulsions. We demonstrate that the spontaneous formation of aqueous drops can be reduced by at least an order of magnitude if appropriate surfactants are employed or if the thickness of double emulsion shells is reduced to dimensions that are of the same order of magnitude as the diameter of the small aqueous drops. These measures significantly reduce cross-contaminations, thereby opening up new possibilities to use drops as vessels for example for conducting high throughput screening assays with a significantly increased accuracy.

## Results and Discussion

### 2.1. Permeability of water-oil-water double emulsions

Water-oil-water double emulsion drops with a diameter of 90 µm and a shell thickness of 12 µm are produced in poly(dimethyl siloxane) (PDMS)-based microfluidic devices[59] that are fabricated using soft lithography,[60] as shown in the optical micrographs in Figures 1a and 1b.

We employ an aqueous solution containing 15 wt.% poly(ethylene glycol) (PEG) 6000 Da and 0.1 wt.% fluorescein sodium salt as an inner phase, a perfluorinated oil, HFE-7500, containing block copolymer surfactants as a middle phase, and an aqueous solution with 10 wt.% poly(vinyl alcohol) (PVA) as an outer phase. PVA is required to impart stability to the double emulsions during their collection and is subsequently removed by thoroughly washing the double emulsions with a PVA-free aqueous solution. To prevent osmotic pressure gradients that would change the dimensions of the double emulsions during their collection and storage, we balance the osmolarities of the two aqueous phases using D-saccharose. To stabilize double emulsion drops, we employ diblock copolymers composed of a perfluorinated block that is covalently linked to a PEG-based hydrophilic block. Alternatively, we stabilize double emulsion drops with triblock copolymers composed of two perfluorinated blocks that are interspaced by a PEG-based block, as shown schematically in Figure 1c.

 

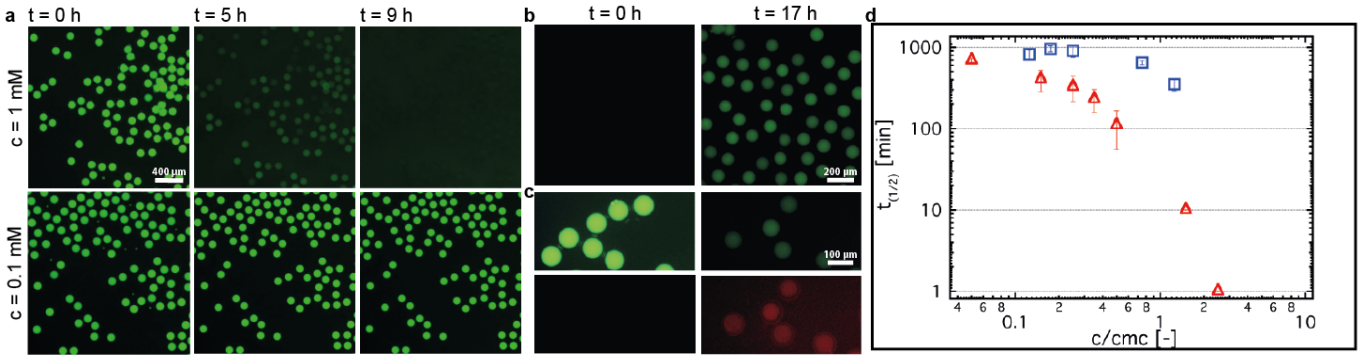


**Fig 2.** Permeability of double emulsions. (a) Time-lapse fluorescent microscope images of double emulsions with 12 µm thick shells containing 1 mM (top) and 0.1 mM (bottom) $FSH_2$-Jeffamine900. (b) Double emulsions stabilized by 1 mM $FSH_2$-Jeffamine600 containing no dye before and after storage in an aqueous solution containing 0.025 wt.% fluorescein. (c) Double emulsions stabilized by 1 mM $FSH_2$-Jeffamine600 containing fluorescein in the core, before and after storage for 17 h in an aqueous solution containing cresyl violet perchlorate. Fluorescein diffuses from the core into the continuous phase whereas cresyl violet perchlorate diffuses from the continuous phase into the core of double emulsions. (d) Time until 50% of fluorescein is released, $t_{1/2}$, as a function of the concentration of $FSH_2$-Jeffamine900 (△) and FSH-Jeffamine1000 (□), contained in the double emulsion shells. The surfactant concentrations are normalized by their respective CMCs.

We systematically change the length of the hydrophilic block to vary the inverse packing parameter, α', of the block copolymer surfactant, defined as the ratio of the cross-sections of the hydrophilic to the hydrophobic tail, $\alpha' = \frac{v}{a_0 l_h}$ ; here $v$ is the volume of the hydrophilic chain, $a_0$ the area of the hydrophobic group, and $l_h$ the length of the hydrophilic block.[61] Because the head group and the tail of our surfactants are polymer blocks, we calculate α' as $\alpha' = \frac{Rg_{(hydrophilic)^2}}{Rg_{(hydrophobic)^2}}$; here $R_g$ is the radius of gyration of the respective block. To account for the fact that triblock copolymers have two hydrophobic blocks, we divide α' of triblock-copolymer surfactants by two and obtain the inverse packing parameters summarized in Table 1.[39]

To maximize the accuracy of screening assays, double emulsions should be impermeable to encapsulants. To test if reagents are transported across the shell of double emulsions, we encapsulate fluorescein and monitor the fluorescence inside the double emulsions as a function of time. The vast majority of fluorescein is released within 7 h if double emulsions are stabilized with 1 mM of the triblock copolymer surfactant $FSH_2$-Jeffamine900, as shown in the top panel of Figure 2a and Movie S1. Similarly, if empty double emulsions are incubated in a fluorescein-containing continuous phase, fluorescein is transported into empty core, as shown in Figure 2b, indicating that reagent exchange occurs in both directions.

To test if this exchange is driven by differences in the chemical potential of the two aqueous phases, we incubate fluorescein-loaded drops in an aqueous solution containing cresyl violet perchlorate. Also in this case, fluorescein diffuses from the double emulsion core into the continuous phase while cresyl violet perchlorate is transported from the continuous phase into the double emulsion core, as shown in Figure 2c. This result indicates that reagents are simultaneously transported into and out of the core of double emulsions. The rate of this transport is pH-dependent, as shown in Figure S1, well in agreement with previous reports. However, because most of the high throughput screening experiments are performed under physiologic conditions, we investigate the permeability of double emulsions at neural pH.

This reagent exchange is remarkable because the solubility of fluorescein in the oil phase is very low, such that this transport cannot be solely explained by diffusion. If the transport of fluorescein across the oil shell was caused by surfactants that form inverse micelles, we would expect this leakage to decrease with decreasing surfactant concentration, by analogy to what has been observed for single emulsion drops.[42,48] In this case, there should be a strong decrease in the leakage, if the surfactant concentration falls below the critical micelle concentration (CMC). To test this hypothesis, we quantify the CMC for each surfactant using interfacial tension and dynamic light scattering (DLS) measurements, as detailed in Figure S2 and summarized in Table 1. We monitor the fluorescence inside double emulsions stabilized with $FSH_2$-Jeffamine900 and quantify the time required to release 50% of the fluorescein, $t_{½}$, as summarized in Figure 2d and detailed in Figure S3. Indeed, the leakiness strongly decreases with decreasing surfactant concentration. However, we still observe a significant leakage, even if the surfactant concentration is below the CMC, as shown by the red triangles in Figure 2d and Movie S1. This finding suggests that other factors might also contribute to the transport of reagents across the oil shell.

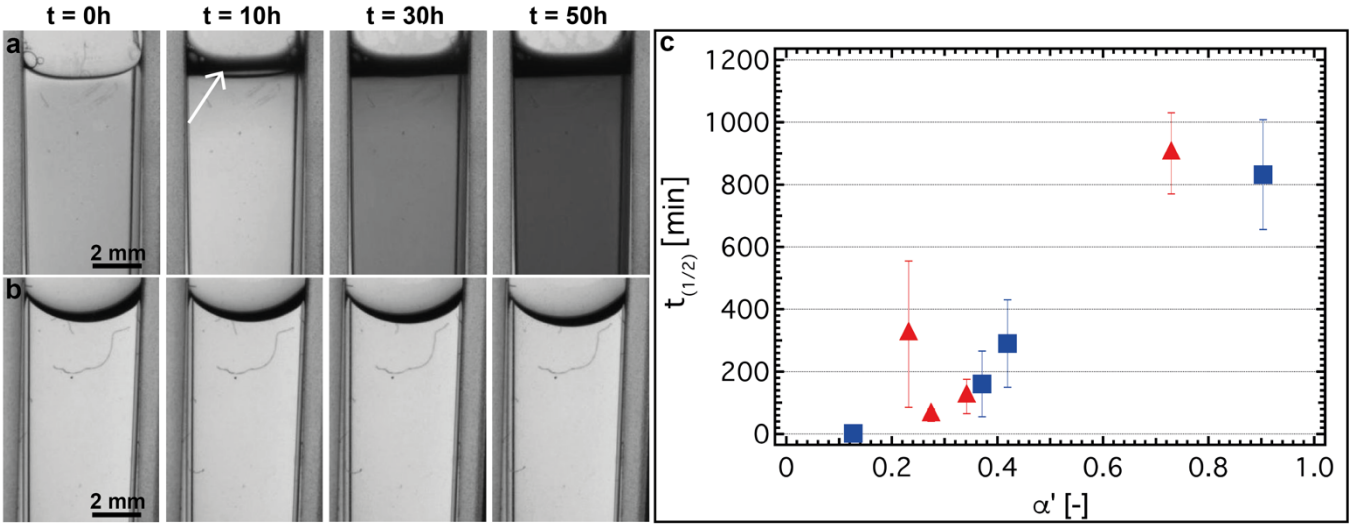


**Fig 3.** Spontaneous formation of small aqueous drops in perfluorinated oils. Time-lapse photographs of fluorinated oil (HFE-7500) (a) without surfactant, (b) with 5 mM $FSH_2$-Jeffamine900. In both cases, the oil is covered with a layer of water. Samples are imaged after 0, 10, 30 and 50 hours. (b) The increase in turbidity observed in the oil phase, that starts in proximity to the liquid-liquid interface, as indicated by the white arrow, can be attributed to the spontaneous formation of aqueous drops. (c) Influence of the inverse packing parameter, α', on the leakage of fluorescein from double emulsions stabilized with 1 mM of diblock (■) or triblock (▲) copolymers.

To exclude that the increase in turbidity is caused by the hydration of the PEG-based blocks contained in the surfactants, we disperse $FSH_2$-Jeffamine2000, a surfactant with a much higher PEG molecular weight than that of $FSH_2$-Jeffamine900, in the oil. The turbidity of this sample remains unchanged even though the oil encompasses an equal molar concentration of $FSH_2$-Jeffamine2000 whose PEG molecular is much higher, as shown in Figure S4. This result indicates that the light scattering observed for samples encompassing $FSH_2$-Jeffamine900 cannot solely be caused by the hydration of PEG. To further test this indication, we quantify the size of the scattering objects with dynamic light scattering (DLS) measurements. This analysis reveals objects with diameters of order 100 nm, a size much larger than that of individual surfactant molecules, as detailed in the Figure S5. These results confirm our hypothesis that the scattering objects are small water drops.

### 2.2. Influence of the interfacial tension on the permeability

If small aqueous drops form in the oil phase, new water-oil interfaces must be produced. This process is energetically expensive. We therefore expect the formation of these drops to decrease with increasing interfacial energy and hence, with increasing interfacial tension. To test this expectation, we analyze the permeability of double emulsions stabilized with an equal concentration of surfactants having different compositions and plot it as a function of the interfacial tension. Indeed, the leakiness decreases with increasing interfacial tension for emulsions stabilized with di- and triblock copolymers, as summarized in Figure 4a. Similarly, if double emulsions are stabilized with the same type of surfactant, their leakiness decreases with decreasing surfactant concentration and hence with increasing interfacial tension, as summarized in Figure 4b.

Our results suggest that with increasing interfacial tension, fewer drops form. This suggestion is well in agreement with the observation that the turbidity of the oil remains unchanged if it contains $FSH_2$-Jeffamine2000, a surfactant that only moderately lowers the interfacial tension, as shown in Figure S4. These results further support our hypothesis that the transport of encapsulants across the shell of double emulsions is mainly caused by aqueous drops that spontaneously form in proximity to the liquid-liquid interface, as schematically illustrated in Figure 4c.

The leakiness of double emulsions can be reduced by increasing the interfacial tension. However, if the interfacial tension is increased, the stability of single emulsion drops usually decreases.[39] This trade-off would limit the use of surfactant stabilized single emulsion drops for high accuracy screening assays. To test, if the stability of double emulsions also inversely scales with the interfacial tension, we quantify their stability by incubating them at 95°C for 10 min. We determine the fraction of double emulsions that remains intact during this incubation using optical microscopy. The majority of double emulsion drops stabilized with any of the tested surfactants remains intact during this incubation, as shown in Figure S6. Remarkably, we cannot observe any clear correlation between the drop stability and the surfactant composition, even though the surfactant composition influences the interfacial tension, as summarized in Table 1. These results suggest that for double emulsions, a good stability must not be traded off with a low permeability such that they have the potential to be well-suited tight vessels for screening assays.

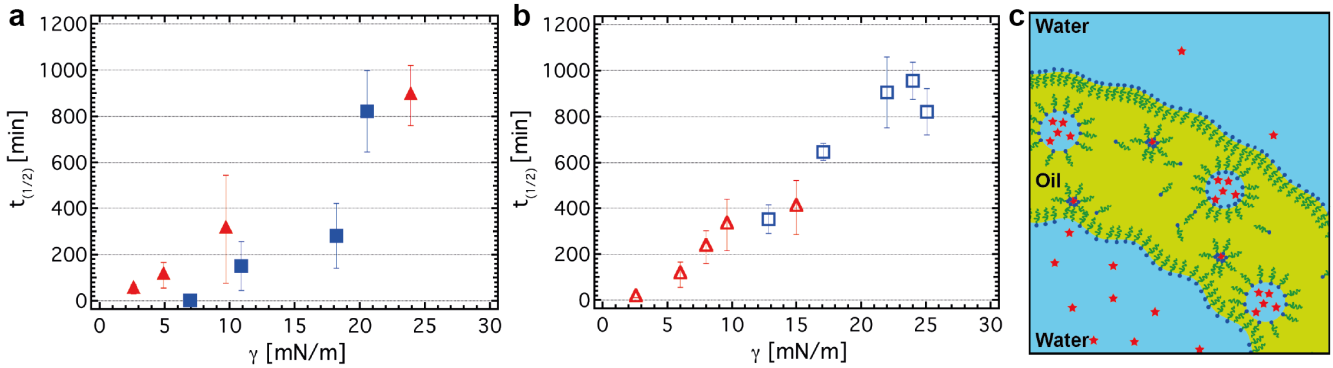


**Fig 4.** Leakage of double emulsions. (a) Influence of the interfacial tension, $\gamma$, on the transport of fluorescein across the oil shell of double emulsions stabilized with 1 mM of diblock (■) and triblock (▲) copolymer surfactants, measured as $t_{1/2}$. (b) Influence of $\gamma$ on $t_{1/2}$ of double emulsion stabilized with different concentrations of $FSH_2$-Jeffamine900 (△) and FSH-Jeffamine1000 (□). (c) Schematic illustration of a water-oil-water double emulsion drop with the suggested mechanism by which encapsulants (red stars) are transported across their oil shell (green): Small aqueous drops (blue) act as carriers for encapsulants.

### 2.3. Influence of surfactant structure on the permeability

Our results indicate that small aqueous drops spontaneously form in close proximity to the liquid-liquid interface. If these drops are formed at the liquid-liquid interface, this interface must deform. Surfactants with small inverse packing parameters increase the local curvature of liquid-liquid interfaces,[64,65] thereby likely facilitating the formation of small drops in the presence of convective flows.[62,63] Indeed, our results suggest that the formation of these drops, and hence the transport of reagents across the oil shell, increases with decreasing inverse packing parameter of the surfactant, as indicated in Figure 3c. Surfactants with small inverse packing parameters also more easily assemble into inverse micelles that can grow into drops, by analogy to emulsion polymerization processes;[66–68] this could be another contributing reason for the spontaneous formation of drops. The exact mechanism by which these small drops form remains to be determined.

**2.4. Transport of large reagents across the oil phase.** If small aqueous drops spontaneously form in the shell of double emulsions, we expect them to also transport large encapsulants across the shell. Many of the drop-based screening assays are employed for biological applications. To test if also biologically relevant encapsulants are transported across oil phases, we load double emulsions with fluorescently labelled single strand DNA composed of 17 base pairs. These DNA strands are rapidly transported across the shell, as shown by the yellow triangle in Figure 5a. Even plasmids containing up to 11000 base pairs are transported across the shell of these double emulsion drops, as shown by the orange circle in Figure 5c. A similar leakage of encapsulants is observed if commercial perfluorinated oil and surfactant solutions are employed, as shown in Figure S7. These results demonstrate that double emulsions are highly permeable also towards large encapsulants. To test if also large solid objects can be transported across the oil phase, we produce double emulsions that contain fluorescently labelled 100 nm diameter polystyrene (PS) beads in their cores; these double emulsions are stabilized with 1 mM $FSH_2$-Jeffamine900, as detailed in Figure S8. Indeed, also these PS beads are transported across the oil shell, as indicated by the decrease in fluorescence over time shown by the microscope image in Figures 5b and c and the blue squares in Figure 5a.

To test if this transport is limited to double emulsions, we produce two batches of water in oil single emulsion drops, one where drops are loaded with PS beads and one with empty drops. Upon mixing of the two batches, the fluorescence of the PS-loaded single emulsion drops decreases over time, as shown in Figure 5c and detailed in the Figure S9. These results indicate that the transport of reagents, that can be as large as 100 nm in diameter, is not limited to oil shells of double emulsions but also occurs across bulk oil phases.

### 2.5. Influence of shell-thickness on permeability

The permeability of double emulsions can be reduced if they are stabilized with an appropriate surfactant. For the system tested here, the triblock copolymer surfactant $FSH_2$-Jeffamine2000 results in the lowest permeability. However, this reduction in permeability requires surfactants that are not commercially available and hence, that are more difficult to access. For many applications, it would be beneficial to reduce the leakiness of double emulsion drops without changing the surfactant composition. If the transport of reagents is caused by 100 nm diameter drops, we expect it to be slowed down if we reduce the shell thickness to values that are similar to those of the diameter of the small drops. To test this expectation, we produce double emulsions with different shell thicknesses; all these double emulsions are stabilized with $FSH_2$-Jeffamine900. To produce double emulsions with shell thicknesses below 4 µm, we employ the microfluidic aspiration device that can reduce the shell thickness of double emulsions down to 330 nm.[69] Indeed, the transport of fluorescein across a shell as thin as 0.33 µm is much slower than that across a 8.4 µm thick shell, as a comparison of time-lapse fluorescence micrographs in Figure 6a and Movie S3 reveals. If the shell thickness is reduced from 13.5 µm to 0.33 µm, $t_{1/2}$ increases from 118 min to 1679 min, as shown in Figure 6b. We assign the decrease in

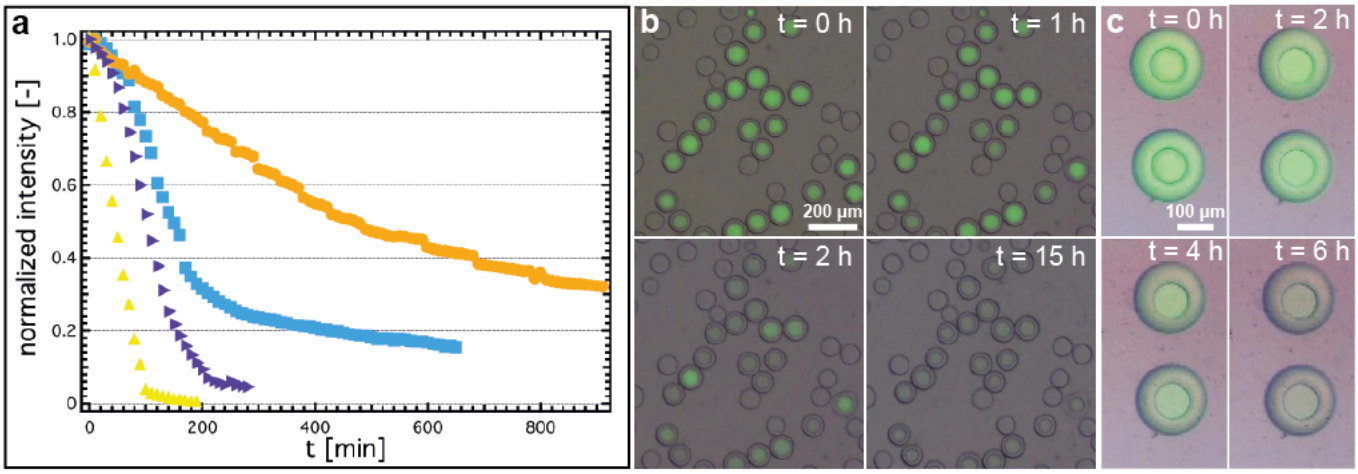


**Fig 5.** Transport of encapsulants across the shell of double emulsions. (a) Normalized fluorescent intensity of the double emulsion cores as a function of the incubation time if the cores contain 100 nm polystyrene beads (■), 11000 base pairs long plasmid (●), 17 base pair long single strand DNA (▲) and fluorescein (▶). All double emulsions are stabilized with 1 mM $FSH_2$-Jeffamine900. (b) Time-lapse fluorescent micrographs of double emulsions stabilized with 1 mM $FSH_2$-Jeffamine900 that encompass fluorescently labelled 100 nm polystyrene beads in their cores. (c) Trapped single emulsion drops containing 100 nm polystyrene beads imaged over time. A decrease in florescence intensity is observed.

permeability to the steric hindrance that delays or even suppresses drop formation. In addition, the thinner shells have a higher hydrodynamic resistance that slows down the convective flow of the oil, thereby reducing the propensity for small aqueous drops to form in proximity of the liquid-liquid interface. These results demonstrate that the permeability of double emulsions can be reduced by more than an order of magnitude without changing the composition of the surfactants by simply reducing the thickness of the oil shell. This reduction in shell thickness constitutes an elegant way to minimize the transport of reagents across the shell of double emulsion drops, and thereby offers new ways to improve the accuracy of screening assays.

## Experimental Section

### Fabrication of the microfluidic device

The microfluidic device was produced from poly(dimethyl siloxane) (PDMS) (Dow Corning, USA) using soft lithography.[60] To produce double emulsions the different channels of the microfluidic device must be surface treated differently. The PDMS device was activated with 1M NaOH solution that was kept in the channels for 10 min before it was removed with compressed air. To render the main channel downstream the 3D junction hydrophilic, we treated it with an aqueous solution containing 2 wt.% polydiallyldimethylammonium chloride (Sigma-Aldrich, USA). To render the injection channels fluorophilic, we treated them with an HFE-based solution containing 2 vol.% of trichloro(1H,1H,2H,2H-perfluorooctyl)silane (Sigma-Aldrich, USA). The solutions were kept in the channels for 30 min before the channels were dried with compressed air.

### Surfactant synthesis

All surfactants were synthesized as described previously.[32,39] In brief, 1 mol equivalent of Krytox FSH 157 (~6500 Da, Chemours, USA) was dissolved at 0.1 g mL-1 in Novec HFE-7100 (3M, USA). The reaction was performed under argon using dry glassware. The carboxylic end group of the Krytox FSH 157 was activated by adding 10 mol equivalent of thionyl chloride (Merck, Germany) and refluxing it at 65°C for 2h. Unreacted thionyl chloride was removed by heating the reaction to 90°C under reduced pressure for 1 hour. After cooling the activated Krytox FSH to room temperature, it was re-dissolved in HFE-7100. To dry the hydrophilic block, 1.1 mol equivalent of the hydrophilic block for diblock copolymers or 0.57 mol equivalent of the hydrophilic block for triblock copolymers was dissolved in trifluoro toluene (Sigma-Aldrich, USA) at 0.1 g mL-1 and heated to 120°C. By slowly reducing the pressure the solvent was evaporated using a bridge connected to a Schlenk flask. To synthesize the diblock copolymer we used monofunctional amine-terminated PEG (Jenkem Mw 295 Da) and Jeffamine (Huntsman M-600, M-1000, M-2005) and for the synthesis of the triblock copolymer we used homobifunctional amine terminated PEG (Jenkem Mw 368) and Jeffamine (Huntsman, Jeffamine ED-600, ED-900, ED-2003). After the majority of the solvent was evaporated and the reaction mixture was cooled to room temperature, anhydrous dichloromethane (Sigma-Aldrich, USA) was added until the PEG was re-dissolved. To drive the reaction to completion, 1.5 mol equivalent of triethylamine (Sigma-Aldrich, USA) was added to the PEG solution. The PEG solution was added to the activated Krytox and refluxed overnight at 65°C. The surfactant was subsequently purified from excess unreacted PEG by dissolving the product in a mixture of methanol (Sigma-Aldrich, USA) and HFE-7100. To separate the surfactant from unreacted PEG, we centrifuged the product at 3000 g and 3°C for 15 min (Mega Star, 1.6R, VWR)

and removed the top layer. This washing step was repeated three times before the surfactant was dried using a rotary evaporator (Hei-VAP, Heidolph, Germany) and a freeze dryer (FreeZone 2.5, Labconco, USA).

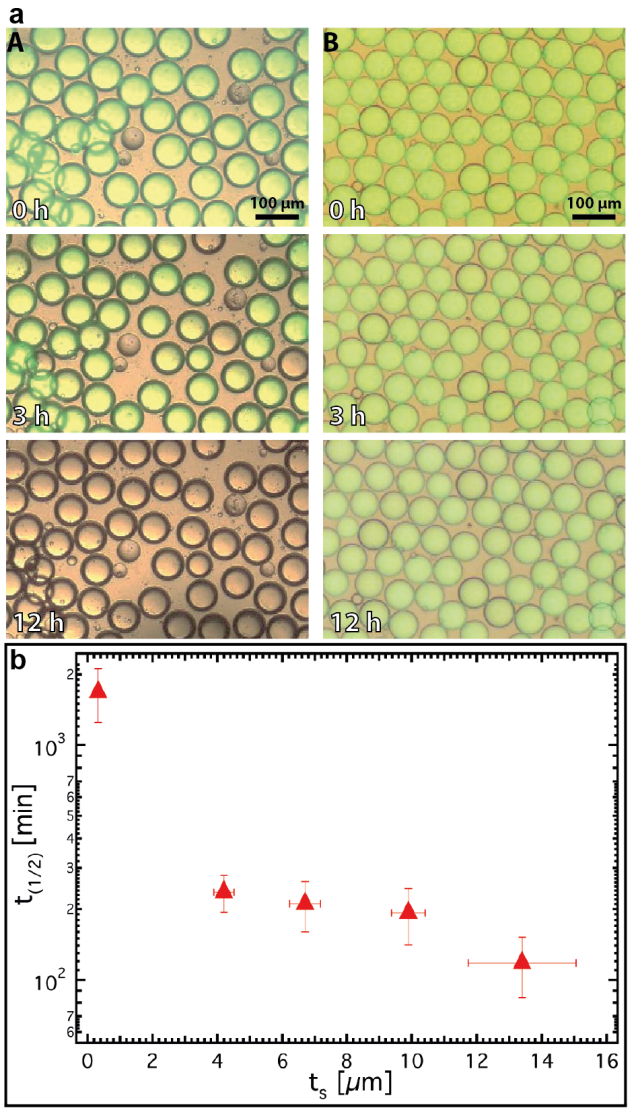


**Fig 6.** Influence of shell thickness on leakiness. (a) Overlay time-lapse optical and fluorescence micrographs of double emulsions whose cores contain fluorescein and whose shell thickness is (A) $t_s$ = 8.4 µm and (B) $t_s$ = 0.33 µm. (b) Influence of the shell thickness, $t_s$, on $t_{1/2}$ for double emulsions stabilized with 1 mM $FSH_2$-Jeffamne900.

### Production of double emulsions

Water-oil-water double emulsions were produced by injecting the liquids with syringe pumps (Cronus Sigma 1000, Labhut, UK). The outer phase was injected at ~6000 µL/h, the middle phase at ~1300 µL/h, and the inner phase at ~1200 µL/h. The inner phase is composed of water containing 15 wt.% PEG with a molecular weight of 6000 Da (Carl Roth, Germany) and 0.1 wt.% fluorescein disodium salt (Carl Roth, Germany). The middle phase is composed of HFE-7500 (0.77 cSt) containing different concentrations of a surfactant. The outer aqueous phase is composed of water containing 10 wt.% polyvinyl alcohol (PVA) 13-18 kDa (Sigma-Aldrich, USA). The osmolarity of the two aqueous phases were measured using an Osmometer (Advanced Instruments, Fiske 210) and matched by adding D(+)-Saccharose (Carl Roth, Germany).

To study the transport of the polystyrene beads, we added FITC-labelled polystyrene beads with a diameter of 100 nm (Nanocs, USA) to an aqueous solution containing 15% PEG 6 kDa and studied the release from double emulsions. For studying the transport of DNA, we used 11000 base pair long pSIN-TRE-GW-3HA plasmid prepared using Qiagen plasmid MIDI kit and concentrated at 1 µg/µL. For the leakage experiment, we stained the plasmid with the SYBR gold double strand specific DNA intercalating dye by adjusting the final concentration on 39X (Invitrogen 10 000X concentrate in DMSO) and we adjusted the plasmid concentration to 12 ng/µL in water and PEG before producing double emulsions. For single stranded DNA leakage experiments we used fluorescein labelled 17 base pair long ssDNA (FAM) ordered from IDT (standard desalting) that was dissolved in distilled water and PEG to 2 µM.

### Production of submicron shell double emulsions

Double emulsions with shells whose thickness is below 1 µm were produced using the microfluidic aspiration device.[69] In brief, double emulsions with diameters of 92 µm and shell thicknesses of 8.4 µm were injected in the microfluidic aspiration device at 900 µL/h. Oil was withdrawn through the shunt channels at a rate of 800 µL/h. To spatially separated double emulsions with thin shells, an additional aqueous phase containing PVA was injected downstream the aspiration section at 800 µL/h.

### Leakage measurements

To minimize the influence of PVA on the transport of encapsulants, double emulsions were washed with an osmotically balanced aqueous solution containing sucrose to remove the PVA. To wash the sample, 10 µL double emulsions was added to 1 ml of water, double emulsions sedimented and the supernatant was removed. This procedure was repeated three times. Double emulsions were added into PDMS wells that have previously been filled with the aqueous washing solution. Wells were sealed with mineral oil (Sigma-Aldrich, USA) to prevent evaporation of the water. Fluorescent microscopy images were recorded every 10 min and analyzed using a custom-made MATLAB code that detects the double emulsions and quantifies the intensity inside each double emulsion over time.

### Quantification of the CMC

The critical micelle concentration (CMC) was measured with dynamic light scattering where the count rate was quantified as a function of the surfactant concentration contained in the fluorinated oil Novec HFE-7500. In addition, the interfacial tension of aqueous drops in HFE-7500 containing different surfactants was quantified with a drop shape analyzer (DSA 30, Krüss, Germany).

**Temperature stability of double emulsions**

To quantify the stability of double emulsions if stored at elevated temperatures, they were added into PDMS wells that have previously been bonded to a glass slide. The double emulsions were imaged at room temperature. The sample was subsequently heated to 95°C for 10 min. After the sample was cooled to room temperature it was again imaged to quantify the percentage of double emulsions that remained intact during the incubation.

## Conclusions

Emulsion drops are frequently employed as reaction vessels to conduct high throughput screening assays. The accuracy of these assays is often compromised by the exchange of reagents contained in different drops that causes cross-contaminations. Here, we demonstrate that the transport of reagents across the oil phase is primarily caused by aqueous drops with diameters of the order of 100 nm that spontaneously form in the oil phase. The propensity of these small drops to form and hence, the leakiness of large emulsion drops can be reduced by at least an order of magnitude if they are stabilized with surfactants that only moderately lower the interfacial tension. Because the stability of double emulsions only weakly depends on the interfacial tension, it must not be traded-off with their leakiness such that mechanically stable double emulsions with a very low permeability can be produced. However, this approach requires optimized surfactants. The leakiness of double emulsions can also be strongly decreased if their shell thickness is reduced to values similar to the diameter of the small drops that spontaneously form in the oil. In this case, the formation of these drops is sterically hindered such that almost no encapsulants are transported across thin oil shells. From these mechanistic insights, design rules for the synthesis of optimized surfactants and emulsion fabrication processes can be derived that offer a tighter control over the leakiness of emulsion drops. This understanding might open up new possibilities to use drop-based screening assays also for applications that require a high accuracy, including applications in pharmacy and food industries.

## Conflicts of interest

There are no conflicts to declare.

## Acknowledgements

The authors would like to thank Dr. Armend Håti for his help with the MATLAB code that allows analysis of the leakage, Dr. Bjoern Schulte for helpful inputs on improving the surfactant synthesis, and Mathias Steinacher for measuring the size of the PS beads using SEM. Additionally, we would like to thank Huntsman (Germany) for providing the Jeffamine Products and Chemours (Switzerland) for providing Krytox FSH 157. GE and AV were financially supported by the Swiss National Science Foundation (SNSF, div. II, grant No. 200021_155997). MB was supported by the Interdisciplinary PhD Fellowship Program of the EPFL School of Life Sciences (awarded to BD and EA).

## References

1 A. J. DeMello, *Nature*, 2006, **442**, 394–402.
2 A. B. Theberge, F. Courtois, Y. Schaerli, M. Fischlechner, C. Abell, F. Hollfelder, and W. T. S. Huck, *Angew. Chemie - Int. Ed.*, 2010, **49**, 5846–5868.
3 J. J. Agresti, E. Antipov, A. R. Abate, A. Keunho, A. C. Rowat, J.-C. Baret, M. Marquez, A. M. Klibanov, A. D. Griffiths, and D. A. Weitz, *Proc. Natl. Acad. Sci.*, 2010, **107**, 4004–4009.
4 D. B. Weibel and G. M. Whitesides, *Curr. Opin. Chem. Biol.*, 2006, **10**, 584–591.
5 V. Taly, B. T. Kelly, and A. D. Griffiths, *ChemBioChem*, 2007, **8**, 263–272.
6 S. Köster, F. E. Angilè, H. Duan, J. J. Agresti, A. Wintner, C. Schmitz, A. C. Rowat, C. A. Merten, D. Pisignano, A. D. Griffiths, and D. A. Weitz, *Lab Chip*, 2008, **8**, 1110–1115.
7 N. Shembekar, C. Chaipan, R. Utharala, and C. A. Merten, *Lab Chip*, 2016, **16**, 1314–1331.
8 M. T. Guo, A. Rotem, J. A. Heyman, and D. A. Weitz, *Lab Chip*, 2012, **12**, 2146–2155.
9 H. F. Chan, S. Ma, J. Tian, and K. W. Leong, *Nanoscale*, 2017, **9**, 3485–3495.
10 A. S. Utada, L.-Y. Chu, A. Fernandez-Nieves, D. R. Link, C. Holtze, and D. A. Weitz, *MRS Bull.*, 2007, **32**, 702–708.
11 E. Amstad, M. Chemama, M. Eggersdorfer, L. R. Arriaga, M. P. Brenner, and D. A. Weitz, *Lab Chip*, 2016, **16**, 4163–4172.
12 A. G. Håti, T. R. Szymborski, M. Steinacher, and E. Amstad, *Lab Chip*, 2018, **18**, 648–654.
13 R. Dangla, E. Fradet, Y. Lopez, and C. N. Baroud, *J. Phys. D. Appl. Phys.*, 2013, **46**, 1–8.
14 H.-H. Jeong, V. R. Yelleswarapu, S. Yadavali, D. Issadore, and D. Lee, *Lab Chip*, 2015, **15**, 4387–4392.
15 N. Mittal, C. Cohen, J. Bibette, and N. Bremond, *Phys. Fluids*, 2014, **26**.
16 J.-C. Baret, O. J. Miller, V. Taly, M. Ryckelynck, A. El-Harrak, L. Frenz, C. Rick, M. L. Samuels, J. B. Hutchison, J. J. Agresti, D. R. Link, D. A. Weitz, and A. D. Griffiths, *Lab Chip*, 2009, **9**, 1850–1858.
17 B. El Debs, R. Utharala, I. V. Balyasnikova, A. D. Griffiths, and C. A. Merten, *Proc. Natl. Acad. Sci.*, 2012, **109**, 11570–11575.
18 S. L. Sjostrom, Y. Bai, M. Huang, Z. Liu, J. Nielsen, H. N. Joensson, and H. Andersson Svahn, *Lab Chip*, 2014, **14**, 806–813.
19 B. L. Wang, A. Ghaderi, H. Zhou, J. Agresti, D. A. Weitz, G. R. Fink, and G. Stephanopoulos, *Nat. Biotechnol.*, 2014, **32**, 473–478.
20 A. M. Klein, L. Mazutis, I. Akartuna, N. Tallapragada, A. Veres, V. Li, L. Peshkin, D. A. Weitz, and M. W. Kirschner, *Cell*, 2015, **161**, 1187–1201.
21 E. Z. Macosko, A. Basu, R. Satija, J. Nemesh, K. Shekhar, M. Goldman, I. Tirosh, A. R. Bialas, N. Kamitaki, E. M. Martersteck, J. J. Trombetta, D. A. Weitz, J. R. Sanes, A. K. Shalek, A. Regev, and S. A. McCarroll, *Cell*, 2015, **161**, 1202–1214.
22 J.-C. Baret, Y. Beck, I. Billas-Massobrio, D. Moras, and A. D. Griffiths, *Chem. Biol.*, 2010, **17**, 528–536.
23 O. J. Miller, A. El Harrak, T. Mangeat, J.-C. Baret, L. Frenz, B. El Debs, E. Mayot, M. L. Samuels, E. K. Rooney, P. Dieu, M. Galvan, D. R. Link, and A. D. Griffiths, *Proc. Natl. Acad. Sci.*, 2012, **109**, 378–383.
24 D. Pekin, Y. Skhiri, J.-C. Baret, D. Le Corre, L. Mazutis, C. Ben Salem, F. Millot, A. El Harrak, J. B. Hutchison, J. W. Larson, D. R. Link, P. Laurent-Puig, A. D. Griffiths, and V. Taly, *Lab Chip*, 2011, **11**, 2156–2166.

 

25 V. Taly, D. Pekin, L. Benhaim, S. K. Kotsopoulos, D. Le Corre, X. Li, I. Atochin, D. R. Link, A. D. Griffiths, K. Pallier, H. Blons, O. Bouché, B. Landi, J. B. Hutchison, and P. Laurent-Puig, *Clin. Chem.*, 2013, **59**, 1722–1731.
26 A. Didelot, S. K. Kotsopoulos, A. Lupo, D. Pekin, X. Li, I. Atochin, P. Srinivasan, Q. Zhong, J. Olson, D. R. Link, P. Laurent-Puig, H. Blons, J. B. Hutchison, and V. Taly, *Clin. Chem.*, 2013, **59**, 815–823.
27 H. Song, D. L. Chen, and R. F. Ismagilov, *Angew. Chemie Int. Ed.*, 2006, **45**, 7336–7356.
28 L. S. Roach, H. Song, and R. F. Ismagilov, *Anal. Chem.*, 2005, **77**, 785–796.
29 K. C. Lowe, *J. Fluor. Chem.*, 2002, **118**, 19–26.
30 K. C. Lowe, *J. Fluor. Chem.*, 2001, **109**, 59–65.
31 J.-C. Baret, *Lab Chip*, 2012, **12**, 422–433.
32 C. Holtze, A. C. Rowat, J. J. Agresti, J. B. Hutchison, F. E. Angilè, C. H. J. Schmitz, S. Köster, H. Duan, K. J. Humphry, R. A. Scanga, J. S. Johnson, D. Pisignano, and D. A. Weitz, *Lab chip*, 2008, **8**, 1632–1639.
33 J. Ng Lee, C. Park, and G. M. Whitesides, *Anal. Chem.*, 2003, **75**, 6544–6554.
34 M. Macris Kiss, L. Ortoleva-Donnelly, N. R. Beer, J. Warner, C. G. Bailey, B. W. Colston, J. M. Rothberg, D. R. Link, and J. H. Leamon, *Anal. Chem.*, 2008, **80**, 8975–8981.
35 L. Rosenfeld, T. Lin, R. Derda, and S. K. Y. Tang, *Microfluid. Nanofluidics*, 2014, **16**, 921–939.
36 D. S. Tawfik and A. D. Griffiths, *Nat. Biotechnol.*, 1998, **16**, 652–656.
37 S.-Y. Teh, R. Lin, L.-H. Hung, and A. P. Lee, *Lab chip*, 2008, **8**, 198–220.
38 R. Seemann, M. Brinkmann, T. Pfohl, and S. Herminghaus, *Reports Prog. Phys.*, 2012, **75**.
39 G. Etienne, M. Kessler, and E. Amstad, *Macromol. Chem. Phys.*, 2017, **218**, 1–10.
40 O. Wagner, J. Thiele, M. Weinhart, L. Mazutis, D. A. Weitz, W. T. S. Huck, and R. Haag, *Lab Chip*, 2015, **16**.
41 J. Chang, Z. Swank, K. Oliver, S. J. Maerkl, and E. Amstad, *Sci. Rep.*, 2018, 1–9.
42 Y. Skhiri, P. Gruner, B. Semin, Q. Brosseau, D. Pekin, L. Mazutis, V. Goust, F. Kleinschmidt, A. El Harrak, J. B. Hutchison, E. Mayot, J.-F. Bartolo, A. D. Griffiths, V. Taly, and J.-C. Baret, *Soft Matter*, 2012, **8**, 10618–10627.
43 G. Woronoff, A. El Harrak, E. Mayot, O. Schicke, O. J. Miller, P. Soumillion, A. D. Griffiths, and M. Ryckelynck, *Anal. Chem.*, 2011, **83**, 2852–2857.
44 Y. Chen, A. W. Gani, and S. K. Y. Tang, *Lab Chip*, 2012, **12**, 5093–5103.
45 P. Gruner, B. Riechers, B. Semin, J. Lim, A. Johnston, K. Short, and J. C. Baret, *Nat. Commun.*, 2016, **7**, 910392.
46 L. Mazutis, J.-C. Baret, P. Treacy, Y. Skhiri, A. F. Araghi, M. Ryckelynck, V. Taly, and A. D. Griffiths, *Lab Chip*, 2009, **9**, 2902–2908.
47 P. R. Marcoux, M. Dupoy, R. Mathey, A. Novelli-Rousseau, V. Heran, S. Morales, F. Rivera, P. L. Joly, J. P. Moy, and F. Mallard, *Colloids Surfaces A Physicochem. Eng. Asp.*, 2011, **377**, 54–62.
48 F. Courtois, L. F. Olguin, G. Whyte, A. B. Theberge, W. T. S. Huck, F. Hollfelder, and C. Abell, *Anal. Chem.*, 2009, **81**, 3008–3016.
49 J. A. Stapleton and J. R. Swartz, *PLoS One*, 2010, **5**.
50 P. A. Sandoz, A. J. Chung, W. M. Weaver, and D. Di Carlo, *Langmuir*, 2014, **30**, 6637–6643.
51 M. Najah, E. Mayot, I. P. Mahendra-Wijaya, A. D. Griffiths, S. Ladame, and A. Drevelle, *Anal. Chem.*, 2013, **85**, 9807–9814.
52 O. Scheler, T. S. Kaminski, A. Ruszczak, and P. Garstecki, *ACS Appl. Mater. Interfaces*, 2016, **8**, 11318–11325.
53 J.-W. Janiesch, M. Weiss, G. Kannenberg, J. Hannabuss, T. Surrey, I. Platzman, and J. P. Spatz, *Anal. Chem.*, 2015, **87**, 2063–2067.
54 M. Pan, L. Rosenfeld, M. Kim, M. Xu, E. Lin, R. Derda, and S. K. Y. Tang, *ACS Appl. Mater. Interfaces*, 2014, **6**, 21446–21453.
55 L. Wen and K. D. Papadopoulos, *Colloids Surfaces A Physicochem. Eng. Asp.*, 2000, **174**, 159–167.
56 J. Bahtz, D. Z. Gunes, E. Hughes, L. Pokorny, F. Riesch, A. Syrbe, P. Fischer, and E. J. Windhab, *Langmuir*, 2015, **31**, 5265–5273.
57 J. Bahtz, D. Z. Gunes, A. Syrbe, N. Mosca, P. Fischer, and E. J. Windhab, *Langmuir*, 2016, **32**, 5787–5795.
58 S. Bochner De Araujo, M. Merola, D. Vlassopoulos, and G. G. Fuller, *Langmuir*, 2017, **33**, 10501–10510.
59 L. R. Arriaga, E. Amstad, and D. A. Weitz, *Lab Chip*, 2015, **15**, 3335–3340.
60 Y. Xia and G. M. Whitesides, *Angew. Chemie Int. Ed.*, 1998, **37**, 550–575.
61 J. N. Israelachvili, *Intermolecular and Surface Forces (Third Edition)*, Elsevier, 2010.
62 J. Santana-Solano, C. M. Quezada, S. Ozuna-Chacón, and J. L. Arauz-Lara, *Colloids Surfaces A Physicochem. Eng. Asp.*, 2012, **399**, 78–82.
63 J. C. Lapez-Montilla, P. E. Herrera-Morales, S. Pandey, and D. O. Shah, *J. Dispers. Sci. Technol.*, 2002, **23**, 219–268.
64 P. Malo De Molina, M. Zhang, A. V. Bayles, and M. E. Helgeson, *Nano Lett.*, 2016, **16**, 7325–7332.
65 M. Zhang, P. T. Corona, N. Ruocco, D. Alvarez, P. Malo de Molina, S. Mitragotri, and M. E. Helgeson, *Langmuir*, 2018, **34**, 978–990.
66 C. S. Chern, *Prog. Polym. Sci.*, 2006, **31**, 443–486.
67 W. D. Harkins, *J. Am. Chem. Soc.*, 1947, **69**, 1428–1444.
68 W. Smith and R. Ewart, *J. Chem. Phys.*, 1948, **16**, 592–599.
69 A. Vian, B. Reuse, and E. Amstad, *Lab Chip*, 2018.